Model predictive active power control of waked ind farms

Vali, Mehdi; Petrović, Vlaho; Boersma, Sjoerd; Van Wingerden, Jan Willem; Pao, L.Y; Kuhn, Martin

DOI
10.23919/ACC.2018.8431391

Publication date
2018

Document Version
Final published version

Published in
Proceedings of the 2018 Annual American Control Conference (ACC 2018)

2018 Annual American Control Conference (ACC)
June 27–29, 2018. Wisconsin Center, Milwaukee, USA

Model Predictive Active Power Control of Waked Wind Farms

Mehdi Vali[1], Vlaho Petrović[1], Sjoerd Boersma[2], Jan-Willem van Wingerden[2], Lucy Y. Pao[3] and Martin Kühn[1]

Abstract— **In this paper, an adjoint-based model predictive control (AMPC) is proposed in order to provide active power control (APC) services of wind farms, even in the presence of problematic wake interactions. The control objective is defined to minimize wind farm power reference tracking error. The non-unique optimal distribution of wind turbine power references is a resulting by-product which can be very informative for other wind farm control methods. The developed predictive controller employs a medium-fidelity 2D dynamic wind farm model to predict wake interactions at hub-height of wind turbines in advance. An adjoint approach as a computationally efficient tool is utilized to compute the gradient for such a large-scale system. The axial induction factor of each wind turbine is considered here as a control variable to influence the overall performance of a wind farm by taking the wake interactions of the wind turbines into account. The performance of the AMPC-based APC is examined for a layout of a 2×3 wind farm in a wake condition through simulation studies. The results show the effectiveness of the proposed approach and introduce some potential studies to improve and extend its performance.**

I. Introduction

Control of turbines in a wind farm is challenging because of their aerodynamic interactions through wakes. The characteristics of a wake are reduced wind speed and increased turbulence. The former reduces the total power production of the farm and the latter leads to a higher dynamic loading on the downstream turbines. Wind farm control has recently received much attention in order to lower the levelized cost of energy, e.g., by minimizing the undesirable effects of wakes on the power production and fatigue loadings of the downwind turbines [1], [2].

The idea to maximize the power production of wind farms in the presence of wakes is to coordinate the control settings of individual turbines, by taking their wake interactions into account. Two common approaches for wake control of wind farms are induction control [3], [4], [5] and wake-steering control [6], [7], [8]. Furthermore, in order to balance power supply with demand, a wind farm plant should respond to grid requirements through control of its power production, the so-called active power control (APC). Aho *et al.* [9], [10] investigate thoroughly providing APC services at the wind turbine level. Fleming *et al.* [11] study the automatic generation control (AGC) type of APC for a wind farm plant, in which the total power production should track a power demand signal provided by the transmission system operator (TSO), and demonstrate the challenge of providing APC services in wake conditions elaborately.

The traditional approach for APC of a wind farm is to distribute the power demand evenly among wind turbines, which are controlled locally for providing their parts, while neglecting their wake impacts on the downstream turbines. This open-loop method yields satisfying power tracking performance only when enough available power exists, e.g., in non-waked conditions of a wind farm or at high ambient wind speeds [11]. van Wingerden *et al.* [12] have extended this approach to incorporate a classical feedback control to improve the power tracking performance of a waked wind farm. The total power production is fed back in order to adjust the pre-selected power set-points, by distributing wake-induced power tracking errors among the wind turbines. However, the optimal collection of the power set-points, considering dynamic wake interactions, is still an open research question.

Shapiro *et al.* [13] present a model-based receding horizon control for the wind farm power demand tracking. The controller relies on a one-dimensional low-fidelity wake model which assumes equal flow velocity for each row of wind turbines within a wind farm. However, this assumption cannot be held when wakes are deflected because of changes in wind direction. In [13], a 5-minute averaged power production of a simulated wind farm, in which the wind turbines operate with the local greedy control setting, is perturbed by an AGC signal for specifying the total demand from the TSO. This power demand might be lower than the available power of the wind farm when it operates at its global optimal point considering wake interactions [3], [4], [5]. Several other studies like [14] have also proposed optimal control solutions, even though the wake interactions are neglected in the optimal control problem.

We are developing a closed-loop wind farm control in order to minimize the undesirable effects of wake interactions. Figure 1 depicts the control architecture of our investigated optimal control framework for waked wind farms, consisting of the following four main elements:

1) a simplified model of the wind farm to capture the dominant waked inflow dynamics [15], [16],
2) an adjoint-based model predictive control (AMPC) to optimally adjust the wind turbine degrees of freedom,

[1] ForWind - Center for Wind Energy Research, Institute of Physics, University of Oldenburg, Küpkersweg 70, 26129 Oldenburg, Germany. mehdi.vali@uni-oldenburg.de

[2] Delft Center for Systems and Control, Delft University of Technology, Mekelweg 2, 2628 CD Delft, The Netherlands.

[3] Department of Electrical, Computer & Energy Engineering, University of Colorado Boulder, USA.

978-1-5386-5428-6/$31.00 ©2018 AACC

e.g., the axial induction factor and yaw angle [17], [18],
3) a state observer for flow field estimation against uncertainties and mismatches [19], [20],
4) a Large Eddy Simulation (LES) model of the wind farm in order to test the performance and realization of the designed controller, under detailed time-varying interactions with boundary layers [21].

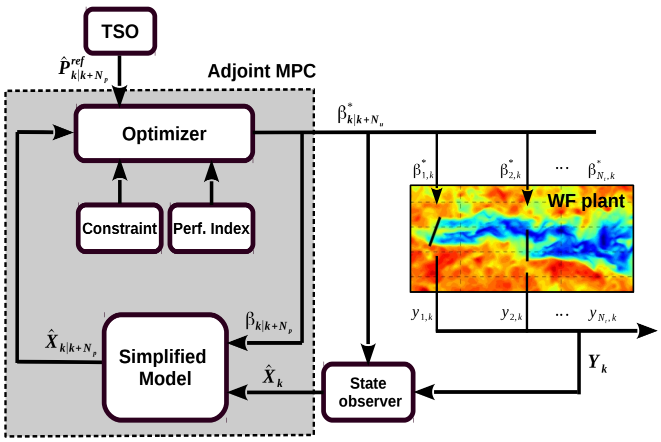

Fig. 1. Schematic illustration of the closed-loop optimal control of wind farms. The grey block contains the main components of the adjoint-based model predictive control (AMPC).

The current paper focuses on the extension of the adjoint-based model predictive control (AMPC) for providing APC services of a waked wind farm. An optimal control problem is formulated for the wind farm power tracking with respect to the axial induction factor of each wind turbine as a control input, taking the wake interactions into account. It employs a two-dimensional dynamic medium-fidelity wind farm model, the so-called WFSim [15], [16], which enables the controller to react to changes in wind direction. We evaluate the performance of the AMPC-based APC for a layout example of a 2×3 wind farm in a wake condition, compared with a baseline controller.

Two important notes for this study are that first, we assume all required state variables X_k for the proposed control approach are measurable (see Fig. 1). Doekemeijer *et al.* [19], [20] have investigated wind field estimation in wind farms, using a limited number of measurement points. Secondly, since the main focus of this contribution is in the optimal control of the wake interactions within a wind farm, we use WFSim as a wind farm plant. In order to test the insensitivity of the AMPC, we perturb the plant with disturbances, e.g., time-varying changes in wind direction, or the controller with imperfect measurements and model mismatches.

The remainder of this paper is organized as follows. In section II, we present briefly the fundamentals of WFSim, a dynamic control-oriented wind farm model. The main focus of section III is on the structure of the proposed AMPC-based APC of waked wind farms. The investigated layout example, the baseline APC, and wake challenges are introduced in section IV. Then, the performance of the AMPC-based APC is discussed through simulation studies for the given wind farm example. Finally, we collect the strengths and weaknesses of the proposed approach in section V as conclusions of this contribution. The potential methods for improving the performance are also outlined.

II. Wind Farm model

This section presents the fundamentals of WFSim [16], which is a control-oriented dynamic medium-fidelity wind farm model. The wind flow is modeled using the incompressible 2D momentum Navier-Stokes equations constrained by the continuity equation [22]:

$$\rho\left(\frac{\partial u}{\partial t}+\nabla\cdot u\mathbf{u}\right)=-\frac{\partial p}{\partial x}+\mu\nabla^2 u+S_x, \tag{1}$$

$$\rho\left(\frac{\partial v}{\partial t}+\nabla\cdot v\mathbf{u}\right)=-\frac{\partial p}{\partial y}+\mu\nabla^2 v, \tag{2}$$

$$\nabla\cdot\mathbf{u}=0, \tag{3}$$

where ρ is the air density, μ is the dynamic viscosity, p is the pressure field and $\mathbf{u}=[u,v]^T$ is the velocity vector field at hub-height. S_x represents the external source terms in the x-direction, which is employed for incorporating the wind turbine models. Equations (1)-(3) are spatially discretized over a staggered grid of $(N_x\times N_y)$ cells. Furthermore, an implicit differencing scheme is employed to discretize the flow model temporally for unsteady solutions.

A wind turbine is modeled using actuator disc theory to exert a thrust force into the incoming flow and extract a certain amount of energy from the wind. The thrust force and the produced power for a single turbine are expressed as follows [23]:

$$F_T=\frac{1}{2}\rho A_d U_\infty^2 C_T(a), \qquad C_T(a)=4a(1-a), \tag{4}$$

$$P_T=\frac{1}{2}\rho A_d U_\infty^3 C_P(a), \qquad C_P(a)=4a(1-a)^2, \tag{5}$$

where U_∞ is the effective wind speed at a far distance upwind from the rotor disc, A_d the swept area of the rotor plane, and C_T and C_P are the thrust and power coefficients of the turbine, respectively, which are functions of the axial induction factor a. The latter is a measure of the decrease in the stream-wise flow velocity at the rotor plane, which is combined with a first-order lag to model the wind turbine dynamic inflow as

$$\dot{a}=\frac{1}{\tau}(a_c-a), \tag{6}$$

where a_c is the wind turbine control command and τ represents the aerodynamic time constant.

Considering the induction effect of a rotor disc as

$$U_d=(1-a)U_\infty \tag{7}$$

enables us to estimate both exerted thrust force and captured power using the measurable wind velocity U_d at the rotor plane and the axial induction factor a. Therefore, the i^{th}

turbine model is incorporated inside the 2D flow model using the following discretized source term:

$$S_{x_i} = -F_{T_i}\frac{\Delta y_i}{A_d} = -2\rho\Delta y_i U_{d_i}^2\beta_i, \tag{8}$$

where Δy_i is the width of the corresponding grid cells where the i^{th} turbine is located and the averaged rotor velocity U_{d_i} is measured. Note that the virtual control variable β_i is defined as

$$\beta_i = \frac{a_i}{1-a_i} \tag{9}$$

to obtain linear expressions of the thrust force and the captured power with respect to the wind turbine control input.

Finally, the wind farm model over a specified staggered grid, containing N_t wind turbines, can be represented in a nonlinear descriptor state-space form as follows

$$E(X_k)X_{k+1} = AX_k + B(X_k)\beta_k + b(X_k), \tag{10}$$

where

$$X_k = \begin{bmatrix}\bar{u}_k\\ \bar{v}_k\\ \bar{p}_k\end{bmatrix}, \quad \beta_k = \begin{bmatrix}\beta_{1,k}\\ \vdots\\ \beta_{N_t,k}\end{bmatrix} \in \mathbb{R}^{N_t\times 1},$$

and $\bar{u}_k \in \mathbb{R}^{(N_x-3)(N_y-2)\times 1}$, $\bar{v}_k \in \mathbb{R}^{(N_x-2)(N_y-3)\times 1}$ and $\bar{p}_k \in \mathbb{R}^{(N_x-2)(N_y-2)\times 1}$ are the vectors that stack all the velocities and pressures in every point of the staggered grid at the time instant k. The matrix $E(X_k)$ represents the spatial discretization terms of the x and y-momentum and the continuity equations (1)-(3). The constant matrix A addresses the temporal discretization of the flow depending on the chosen sampling time. The matrix $B(X_k)$ represents the linear expression of the thrust force with respect to the virtual control input β_k. Finally the matrix $b(X_k)$ represents the effect of the zero stress boundary conditions. The reader is referred to [15], [16] for more details on WFSim and to [17] for implementation of a wind turbine as an actuator disc.

III. Model predictive active power control of wind farms

The adjoint-based model predictive control (AMPC) of wind farms [17], [18] is extended here for providing APC services. The grey box of Fig. 1 contains the main components of the developed AMPC-based APC. The control objective is defined here as the optimal distribution of wind turbine power references, while the sum of the actual turbine power productions follows the wind farm power command, provided by the TSO. The predictive controller relies on a constrained optimization problem, subjected to the control-oriented wind farm model. It contains three main generic steps: prediction, solving the optimization problem over a finite prediction horizon N_p, and implementing the optimal control solutions $\beta_k^\star$ over the receding time horizon $N_u < N_p$. The whole procedure is repeated with new measurements, providing feedback into the optimization problem, which enables the controller to react to varying atmospheric and operating conditions.

A. Optimal control problem

The optimization problem is formulated as minimizing the wind farm power tracking error over a finite time prediction horizon N_p. Hence, we first define the following performance index:

$$\mathscr{J}_k(X_k,\beta_k) = \left(P_k^{\text{ref}} - \sum_{i=1}^{N_t} P_{i,k}\right)^2, \tag{11}$$

addressing the square of wind farm power tracking error with N_t wind turbines, at time instant k. The manipulating variables are the wind turbine induction factors $\beta_k = [\beta_{1,k},\beta_{2,k},\ldots,\beta_{N_t,k}]^T \in \mathbb{R}^{N_t\times 1}$. Note that there exists some redundancy among the control inputs in that multiple solutions $\beta_k^\star$ can lead to the same wind farm tracking error. This flexibility can be used for additional wind farm control objectives, e.g., optimal load distribution among wind turbines.

We regard the discrete-time nonlinear descriptor dynamic system (10) as the simplified wind farm model to predict the responses in advance. We want to find an optimal feedback control law $\beta_k^\star$ so that the system remains feasible and minimizes the average cost of interest, e.g., wind farm power tracking error, over the prediction horizon N_p. The optimization MPC scheme we propose solves, for each current system state X_k, the following constrained optimal control problem:

$$\min_{\tilde{\beta}} \quad \mathscr{J}(\tilde{X},\tilde{\beta}) = \sum_{k=1}^{N_p}\mathscr{J}_k(X_k,\beta_k) + \Delta\beta_k^T\mathbf{R}\Delta\beta_k, \tag{12}$$

$$\text{s.t.} \quad \tilde{\mathbf{C}}(\tilde{X},\tilde{\beta}) = 0, \tag{13}$$

$$0 \le \beta_{i,k} \le \frac{1}{2}, \quad \text{i.e.,} \quad 0 \le a_{i,k} \le \frac{1}{3}, \tag{14}$$

where the first part of (12) describes the active power control goal and the second term represents the quadratic integral criterion of control inputs with $\Delta\beta_k = \beta_k - \beta_{k-1}$. This standard criterion provides an assessment for deviation of the control input. The weighting matrix $\mathbf{R}$ is introduced to penalize the control efforts for a smooth and realizable induction control of wind turbines. The equality constraint (13) represents the wind farm model (10), which evolves over the prediction time horizon N_p, with the following expanded form

$$\tilde{\mathbf{C}} = \begin{bmatrix} C_1(X_0,X_1,\beta_0)\\ C_2(X_1,X_2,\beta_1)\\ \vdots\\ C_{N_p}(X_{N_p-1},X_{N_p},\beta_{N_p-1})\end{bmatrix}, \ \tilde{X} = \begin{bmatrix}X_1\\ X_2\\ \vdots\\ X_{N_p}\end{bmatrix}, \ \tilde{\beta} = \begin{bmatrix}\beta_1\\ \beta_2\\ \vdots\\ \beta_{N_p}\end{bmatrix},$$

It should be noted that (13) represents the wake interactions and their couplings with the axial induction factors over the whole prediction time horizon N_p, which allows us to include them in the optimal control problem. Furthermore, the inequality constraint (14) represents practical constraints on the wind turbine control inputs, where $\beta_{i,k} = \frac{1}{2}$ (i.e., $a_{i,k} = \frac{1}{3}$) corresponds with the Betz limit [23] of the maximum extractable power of an isolated wind turbine.

The optimal control problem is solved iteratively at each prediction window [24]. Given an estimated control variable $\tilde{\beta}^{(n)} \in \mathbb{R}^{N_tN_p\times 1}$ at the n^{th} optimization iteration, a new estimation is determined using the gradient of (12)-(14) as follows

$$\tilde{\beta}^{(n+1)} = \tilde{\beta}^{(n)} - \alpha \left(\nabla_{\tilde{\beta}}^{(n)} \mathscr{J} \right)^T, \tag{15}$$

with α being the step size along a given search direction, which is determined iteratively via a line search method.

B. Adjoint-based gradient of the cost function

Using common approaches, e.g., finite difference method, makes the computation of the gradient intractable and impractical for real-time applications. Adjoint methods give an efficient way to obtain the gradient of a performance index when having many decision variables without tedious calculation of the derivatives of the flow solution with respect to the control variables ($\tilde{X}_{\tilde{\beta}}$). Therefore, the gradient of the performance index can be expressed as [17], [18]:

$$\nabla_{\tilde{\beta}} \mathscr{J} = \mathscr{J}_{\tilde{\beta}}(\tilde{X},\tilde{\beta}) + \Lambda^T \tilde{\mathbf{C}}_{\tilde{\beta}}(\tilde{X},\tilde{\beta}), \tag{16}$$

using the adjoint equation [25]

$$\tilde{\mathbf{C}}_{\tilde{X}}^T(\tilde{X},\tilde{\beta})\Lambda = -\mathscr{J}_{\tilde{X}}^T(\tilde{X},\tilde{\beta}) \tag{17}$$

with $\Lambda = [\lambda_1, \lambda_2, ..., \lambda_{N_p}]^T$ being the adjoint variable and $(.)_{\tilde{X}}$ and $(.)_{\tilde{\beta}}$ representing the partial derivatives of the model and the performance index with respect to $\tilde{X}$ and $\tilde{\beta}$, respectively. The structure of the matrices $\tilde{\mathbf{C}}_{\tilde{X}}$ and $\tilde{\mathbf{C}}_{\tilde{\beta}}$ allows us to derive the dynamic propagation of the adjoint variable and the adjoint-based gradient (16) backward in time [18].

An active set method is employed to enforce the inequality constraint (14) to maintain the applied control inputs within the practical constraints of the wind turbines. The computational efficiency benefits from the sparsity in the system matrices of WFSim. An analysis of the computational complexity of the AMPC can be found in [26].

IV. Simulation Studies

The performance of the proposed model predictive active power control is discussed here through simulation studies with WFSim. This study focuses on a simulation scenario, in which the wake interactions are problematic for a good wind farm power tracking performance, similar to [11], [12]. Note that the APC of wind farms in a non-waked condition simplifies the control problem to a standard tracking one [11], which is not addressed here.

A. Case study and optimal operational point

A layout of a 2×3 wind farm is considered (see Fig. 2) and simulated with WFSim. The wind turbines with rotor diameter $D = 126$ m are spaced $5D$ in the stream-wise direction. The rotor centers of the middle turbines are offset half a rotor diameter from the centers of the upwind and downwind turbines. We have a field of 3000×2000 m^2, i.e., approximately $24D \times 16D$, with a staggered grid of 100×75 cells ($N_x \times N_y$). The simulation is started with an uniform wind field with velocity $u = 10$ m/s and wind direction 8°.

Figure 3 shows the optimal axial induction factors of the wind turbines, achieved using a Game Theoretic approach [3]. Compared with the local greedy control setting

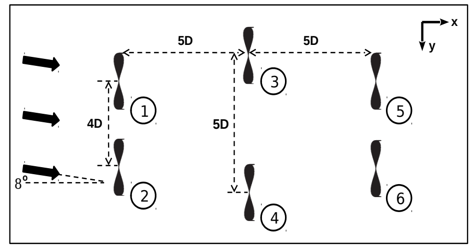

Fig. 2. The layout of the simulated 2×3 wind farm.

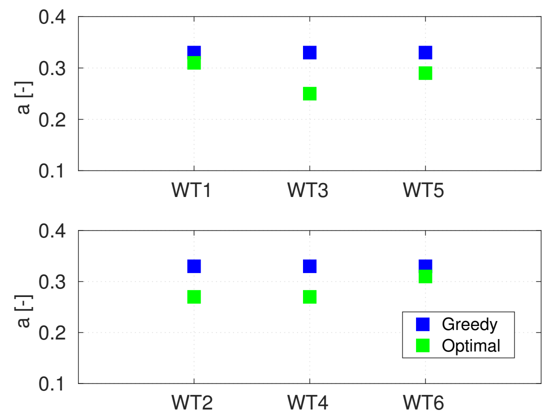

Fig. 3. Optimal axial induction factors of the simulated wind farm example, corresponding to the maximal energy extraction $P_{\text{farm}}^{\max}$. The greedy control setting $a = 0.33$ represents the locally optimal induction of an individual wind turbine.

($a_i = 0.33$), some individual wind turbines are operating at lower power production levels. However, the total wind farm power production is maximized because of the optimal propagation of wakes. Note that the asymmetric distribution of the optimal induction factors at each wind turbine row originates from wake deflections because of the 8° misalignment of the incoming wind with the rotor discs.

The following simulation scenario is defined to evaluate the APC performance. The wind farm starts operating with the optimal axial induction factors (see Fig. 3). After inflow propagation and wake interactions, the APC is activated at time instant 600 s. The simulation sample time and the aerodynamic time constant of each turbine are selected as $\Delta t = 2$ s and $\tau = 13.5$ s [27], respectively.

Moreover, unlike [13] we use the maximal available power $P_{\text{farm}}^{\max}$ instead of averaged power production with local greedy control settings for specifying an AGC-based power demand signal, making the APC of waked wind farms more challenging. Figure 4 depicts the normalized RegD type of an AGC signal, the most rapidly actuating test signal which is used for APC qualification by a regional transmission organization [28]. The time-varying wind farm power command is defined as:

$$P_k^{\text{ref}} = P_{\text{farm}}^{\max} \left(0.9 + 0.1 n_k^{\text{AGC}} \right), \tag{18}$$

where normalized n^{AGC} is simulated according to Fig.4.

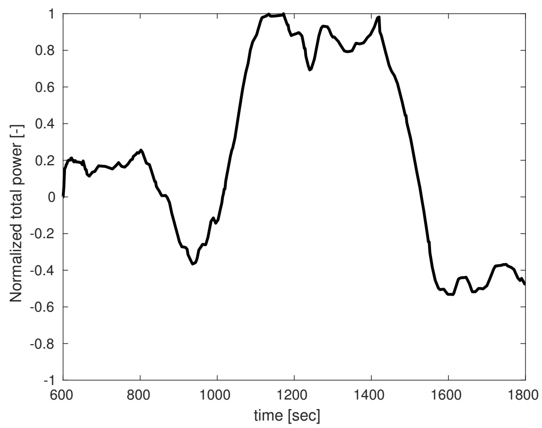

Fig. 4. Normalized RegD type of an AGC test signal [28].

B. Baseline APC and wake challenge

A central open-loop control system, which is studied in [11], is considered here as a baseline APC to share an AGC power signal among the wind turbines. Two different power set-point cases are chosen here. The corresponding fractions of the required AGC response for all six turbines are listed in Table I. The first is based on the traditional APC idea that all wind turbines are de-rated equally. The second uneven distribution is introduced here to illustrate the necessity of considering the wake interactions in the control problem. Hence, several different reserve levels are examined to tune the power set-points of the second baseline for a better wind farm power tracking performance. The lowest power set-points are dedicated to the 4th and 5th wind turbines because they operate fully waked in this case study. Note that the sum of the individual turbine power references for both cases is the same as the demanded power from the TSO.

TABLE I
BASELINE APC POWER RESERVE DISTRIBUTIONS.

	WT1	WT3	WT5
Baseline 1	$1/6$	$1/6$	$1/6$
Baseline 2	$11/48$	$1/6$	$1/12$
	WT2	**WT4**	**WT6**
Baseline 1	$1/6$	$1/6$	$1/6$
Baseline 2	$5/24$	$5/48$	$5/24$

Figure 5 plots the distributed power references among all six turbines along with their actual power productions with both cases of pre-selected baseline set-points. The powers are normalized with respect to $P_{\text{farm}}^{\text{max}}$. Note that each wind turbine has its own feedback controller to locally adjust its own axial induction factor, which can be translated to practical torque and pitch controllers, for following a commanded power reference from a central APC. In the first baseline case, it can be seen that the 4$^{\text{th}}$ and 5$^{\text{th}}$ wind turbines are not capable of following the required AGC response (see blue curves) because of the wake impact by their upwind turbines. Hence, the wind farm power supply cannot be balanced, as shown in Fig. 6. The wind farm power tracking error can be improved with the second baseline APC (see green curves) for this specific case study. Although the power set-points are tuned to minimize the power tracking error, the 5th wind turbine still cannot track its power reference due to the operation inside the wake. Indeed, they should also be adjusted with time-varying changes in atmospheric conditions using feedback control. All in all, it is evident that providing a high-quality AGC response in a wake condition is a challenging control task, which demands an advanced control methodology such as the proposed AMPC.

C. AMPC-based active power control performance

In this section, the performance of the AMPC-based APC for an optimal distribution of a rapidly actuating AGC power

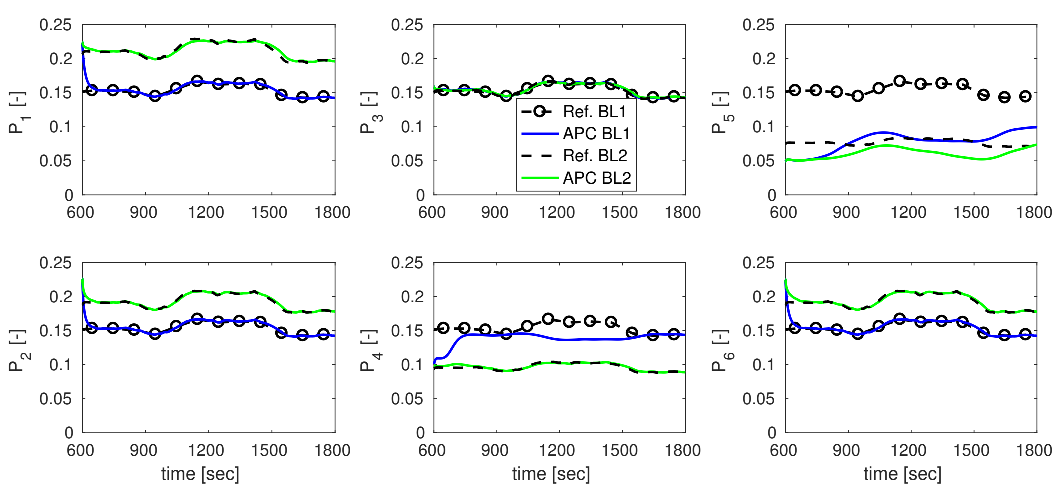

Fig. 5. Normalized power production of the individual wind turbines with the baseline APCs in order to illustrate the challenges of the wake interactions. The powers are normalized with respect to $P_{\text{farm}}^{\text{max}}$. The APC curves are attempting to track their corresponding Ref. trajectories.

signal in a waked condition is illustrated and compared with both baseline cases. The key parameters of the AMPC are chosen here as the prediction horizon $N_p = 200\,\mathrm{s}$ and the receding horizon $N_u = 60\,\mathrm{s}$. The prediction horizon N_p should be long enough to predict the inflow and wake propagation within the given wind farm, while the controller sample time N_u depends on how fast the wind farm dynamics change. The weighting matrix on the control effort is chosen as $R = 0.5I_{[6]}$ in order to avoid high changes of the axial induction factors, where I is the identity matrix with its dimension being the number of wind turbines. Furthermore, it is assumed here that the AGC power demand signal can be predicted reasonably 200 s ahead of time at each measurement point of the controller. Future work will investigate algorithms for predicting AGC signals.

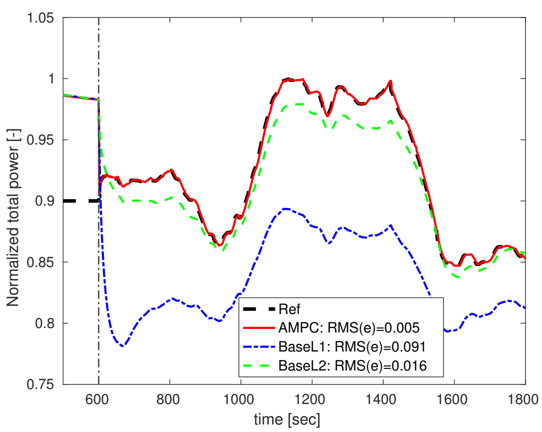

Fig. 6. Normalized total power of the wind farm with the AMPC-based APC, compared with the baseline APCs. The power is normalized with respect to $P^{\max}_{\mathrm{farm}}$. The accuracy of the APCs is compared using the root mean square (RMS) of the tracking errors.

Figure 6 shows the AGC responses of our simulated example. The normalized total power production of AMPC-based APC is compared with the baseline open-loop distributions described above (see Table I). The accuracy of the APC approaches is assessed using the root mean square (RMS) of the wind farm power tracking errors over the whole controlled simulation run-time. It can be seen that the AMPC is capable of optimally regulating the wind turbine power production to enable the total wind farm power to follow the time-varying power demand. Contrary to the aforementioned baseline APCs, the AMPC-based APC takes advantage of the feedback and wake interactions model for optimally adjusting the power references of the wind turbines.

Figure 7 illustrates the individual wind turbine contributions to the wind farm power tracking performance with all the investigated APC cases. The AMPC shows how the AGC power signal should be distributed among the wind turbines in order to address the wake effects. Indeed, the upwind turbines regulate their own impacts on the downwind machines to achieve a good wind farm tracking needed for APC services.

Figure 8 illustrates the axial induction factor trajectories of the individual wind turbines for all the simulated AGC responses. Looking at the first baseline APC performance (blue curves) reveals that the 4$^{\text{th}}$ and 5$^{\text{th}}$ wind turbines are operating at their local optimum point $a = 0.33$ to capture the most possible kinetic energy from the incoming wind. As discussed before, due to wake effects from their upwind turbine there is not enough wind power available to allow the 4$^{\text{th}}$ and 5$^{\text{th}}$ turbines to follow their commanded power references in the first baseline case. Note that the same happens only to the 5$^{\text{th}}$ turbine with the second baseline APC due to a different power set-point selection (see Table I). However, the AMPC finds the optimal wind turbine control trajectories, which regulate wake interactions among wind turbines for a good wind farm power tracking performance.

In addition to the balance of power supply with demand, one desirable APC service for wind farm operators is optimal coordination of dynamic loadings on wind turbines in order

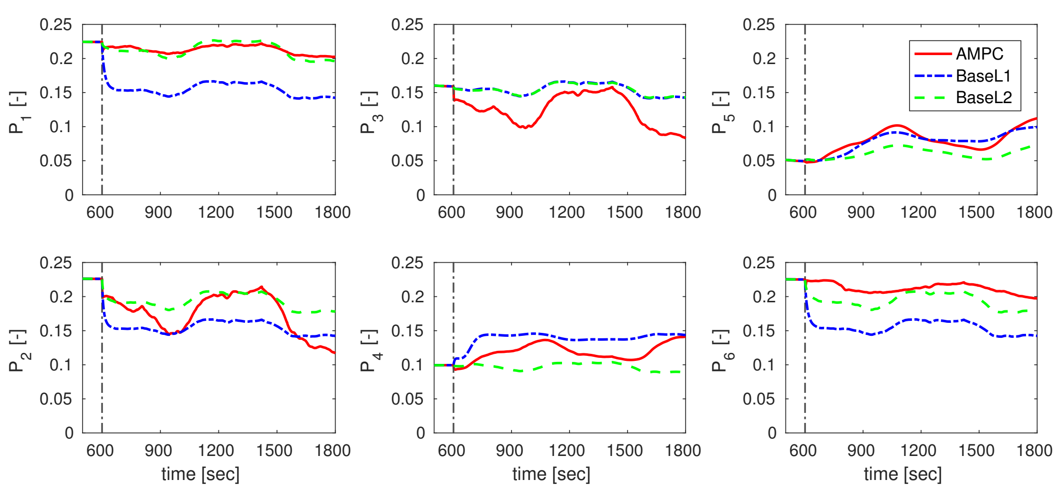

Fig. 7. Normalized power production of the individual wind turbines with the AMPC-based APC, compared with the baseline APCs. The power is normalized with respect to $P^{\max}_{\mathrm{farm}}$.

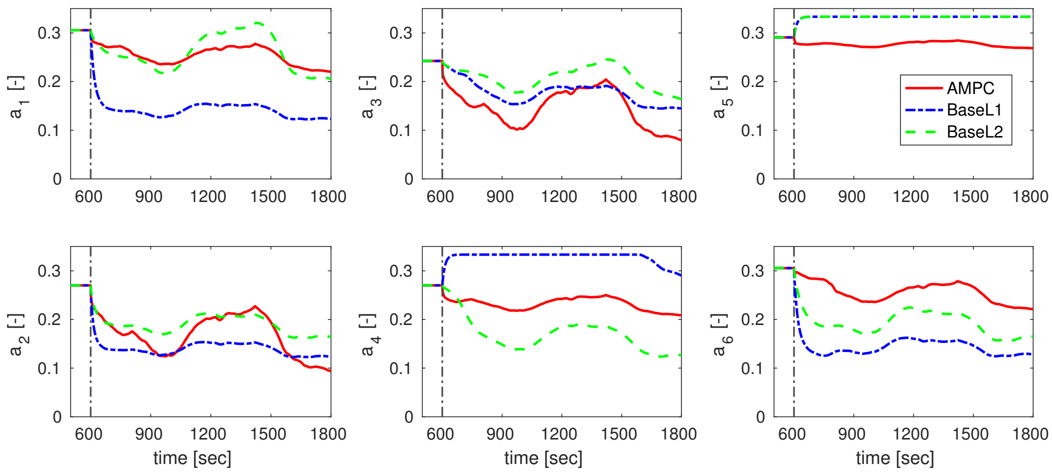

Fig. 8. Axial induction factor trajectories of the individual wind turbines with the AMPC-based APC, compared with the baseline APCs.

to prolong their operational lifespan. The flexibility of the APC of wind farms has been discussed in [14], [12], which can be exploited for minimization of the aggregate fatigue loadings on wind turbines within a wind farm. The AMPC-based APC seems promising for achieving this goal due to the systematic formulation of an optimal control problem, and this is an area of future work in the adjoint-based model predictive control of wind farms.

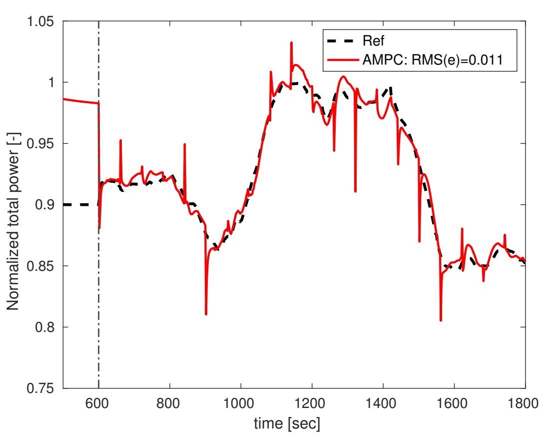

Fig. 9. Normalized total power of the wind farm with the AMPC-based APC with imperfect measurements and a shorter preview of the power demand.

At the end, we demonstrate the sensitivity of the AMPC to some sources of uncertainties. So far, the optimal control problem has been subjected to the dynamic wake interactions of wind turbines. The reaction of the AMPC to slow disturbances like time-varying changes in wind direction is demonstrated in [18] and not repeated here. At each control sample time, the wind farm responses to the control inputs and disturbances, are fed back and then the optimal control inputs are adjusted by analyzing new measurements. Here, we assess the sensitivity of the AMPC-based APC to imperfect measurements. Therefore, all the measured velocity fields $\mathbf{u} = [u, v]^T$ are perturbed with random values, which are bounded by [-1,1] m/s. Moreover, we shorten the preview knowledge of the AGC signal to the first 60 s of the prediction horizon N_p, equal to the chosen wind farm controller sample time N_u. It is assumed that the signal remains constant for the rest of the prediction window N_p.

Figure 9 illustrates the performance of the proposed APC subjected to imperfect measurements and a shorter preview of the demand. It can be seen that the AMPC still provides APC services with a good power tracking precision. The large transients at the beginning of each controller sample time are because of relatively high values of simulated noises with respect to the measured velocity fields, which can be reduced by increasing the weighting matrix $\mathbf{R}$ and as a result slows the rate of change of the wind turbines control inputs.

V. Conclusions and Future Work

An adjoint-based model predictive control, the so-called AMPC, is proposed for providing active power control services of waked wind farms. The wake challenge for wind farm power tracking performance is elaborated first. The optimal control problem is formulated to minimize power reference tracking errors over a prediction horizon, subjected to a dynamic wind farm model. Hence, the AMPC is capable of optimally regulating the specified performance of interest by taking the wake interactions into account. The controller benefits from an adjoint approach as a computationally-efficient tool for computing the gradient. The optimal solutions are adjusted at each measurement point based on the feedback. Hence, contrary to open-loop approaches, it is capable of reacting to varying atmospheric and operating conditions. The effectiveness of the AMPC-based APC is examined using a layout example of a 2×3 wind farm in a wake condition with imperfect measurements. Simulation results show that the AMPC optimally commands the wind turbines, while the total power productions of the wind farm follows the demanded time-varying AGC power signal from the TSO.

In the future, we will implement the AMPC over a Large Eddy Simulation (LES) model of a wind farm in order to examine its performance under more detailed interactions with boundary layers. Furthermore, The AMPC-based APC of wind farms has multiple optimizing solutions with respect to the control inputs, which might be used for providing additional services, e.g., an optimal load coordination of wind turbines.

ACKNOWLEDGMENT

This work has been funded by the German Ministry of Economic Affairs and Energy (BMWi) in the scope of the WIMS-Cluster project (FKZ 0324005) and by the European Union's Seventh Framework Programme for research in the scope of the IRPWind project (No. 609795). Support from a fellowship from the Hanse-Wissenschaftskolleg in Delmenhorst, Germany is also gratefully acknowledged.

REFERENCES

[1] T. Knudsen, T. Bak, and M. Svenstrup, "Survey of wind farm control: power and fatigue optimization," *Wind Energy*, vol. 18, no. 8, pp. 1333–1351, 2015.

[2] S. Boersma, B. M. Doekemeijer, P. M. O. Gebraad, P. A. Fleming, J. Annoni, A. K. Scholbrock, J. A. Frederik, and J. W. van Wingerden, "A tutorial on control-oriented modeling and control of wind farms," in *American Control Conference (ACC)*, May 2017, pp. 1–18.

[3] J. R. Marden, S. D. Ruben, and L. Y. Pao, "A model-free approach to wind farm control using game theoretic methods," *IEEE Transactions on Control Systems Technology*, vol. 21, no. 4, pp. 1207–1214, July 2013.

[4] J. P. Goit and J. Meyers, "Optimal control of energy extraction in wind-farm boundary layers," *Journal of Fluid Mechanics*, vol. 768, pp. 5–50, 2015.

[5] U. Ciri, M. A. Rotea, and S. Leonardi, "Model-free control of wind farms: A comparative study between individual and coordinated extremum seeking," *Renewable Energy*, vol. 113, pp. 1033 – 1045, 2017.

[6] P. M. O. Gebraad, F. W. Teeuwisse, J. W. van Wingerden, P. A. Fleming, S. D. Ruben, J. R. Marden, and L. Y. Pao, "Wind plant power optimization through yaw control using a parametric model for wake effects: a CFD simulation study," *Wind Energy*, vol. 19, no. 1, pp. 95–114, 2016, we.1822.

[7] F. Campagnolo, V. Petrović, J. Schreiber, E. M. Nanos, A. Croce, and C. L. Bottasso, "Wind tunnel testing of a closed-loop wake deflection controller for wind farm power maximization," *Journal of Physics: Conference Series*, vol. 753, no. 3, p. 032006, 2016.

[8] J. Annoni, A. Scholbrock, M. Churchfield, and P. Fleming, "Evaluating tilt for wind plants," in *American Control Conference (ACC)*, May 2017, pp. 717–722.

[9] J. Aho, A. Buckspan, J. Laks, P. A. Fleming, Y. Jeong, F. Dunne, M. Churchfield, L. Y. Pao, and K. Johnson, "A tutorial of wind turbine control for supporting grid frequency through active power control," in *American Control Conference (ACC)*, June 2012, pp. 3120–3131.

[10] J. Aho, P. A. Fleming, and L. Y. Pao, "Active power control of wind turbines for ancillary services: A comparison of pitch and torque control methodologies," in *American Control Conference (ACC)*, July 2016, pp. 1407–1412.

[11] P. A. Fleming, J. Aho, P. Gebraad, L. Y. Pao, and Y. Zhang, "Computational fluid dynamics simulation study of active power control in wind plants," in *American Control Conference (ACC)*, July 2016, pp. 1413–1420.

[12] J.-W. van Wingerden, L. Pao, J. Aho, and P. Fleming, "Active power control of waked wind farms." *IFAC-PapersOnLine*, vol. 50, no. 1, pp. 4484 – 4491, 2017.

[13] C. R. Shapiro, P. Bauweraerts, J. Meyers, C. Meneveau, and D. F. Gayme, "Model-based receding horizon control of wind farms for secondary frequency regulation," *Wind Energy*, vol. 20, no. 7, pp. 1261–1275, 2017, we.2093.

[14] D. Madjidian, "Scalable minimum fatigue control of dispatchable wind farms," *Wind Energy*, vol. 19, no. 10, pp. 1933–1944, 2016, we.1960.

[15] S. Boersma, M. Vali, M. Kühn, and J. W. van Wingerden, "Quasi linear parameter varying modeling for wind farm control using the 2D Navier-Stokes equations," in *American Control Conference (ACC)*, July 2016, pp. 4409–4414.

[16] S. Boersma, P. Gebraad, M. Vali, B. Doekemeijer, and J. W. van Wingerden, "A control-oriented dynamic wind farm flow model: WFSim," *Journal of Physics: Conference Series*, vol. 753, no. 3, p. 032005, 2016.

[17] M. Vali, J. W. van Wingerden, S. Boersma, V. Petrović, and M. Kühn, "A predictive control framework for optimal energy extraction of wind farms," *Journal of Physics: Conference Series*, vol. 753, no. 5, p. 052013, 2016.

[18] M. Vali, V. Petrović, S. Boersma, J.-W. van Wingerden, and M. Kühn, "Adjoint-based model predictive control of wind farms: Beyond the quasi steady-state power maximization." *IFAC-PapersOnLine*, vol. 50, no. 1, pp. 4510 – 4515, 2017.

[19] B. M. Doekemeijer, J. W. van Wingerden, S. Boersma, and L. Y. Pao, "Enhanced Kalman filtering for a 2D CFD NS wind farm flow model," *Journal of Physics: Conference Series*, vol. 753, no. 5, p. 052015, 2016.

[20] B. M. Doekemeijer, S. Boersma, L. Y. Pao, and J. W. van Wingerden, "Ensemble Kalman filtering for wind field estimation in wind farms," in *American Control Conference (ACC)*, May 2017, pp. 19–24.

[21] M. Vali, L. Vollmer, V. Petrović, and M. Kühn, "A closed-loop wind farm control framework for maximization of wind farm power production," in *Wind Energy Science Conference (WESC)*, June 2017.

[22] H. K. Versteeg and W. Malalasekera, *An introduction to computational fluid dynamics: the finite volume method*. Pearson Education, 2007.

[23] R. Gasch and J. Twele, *Wind power plants: fundamentals, design, construction and operation*. Springer Science & Business Media, 2011.

[24] D. P. Bertsekas, *Nonlinear programming*. Athena Scientific Belmont, 1999.

[25] R. Roth and S. Ulbrich, "A discrete adjoint approach for the optimization of unsteady turbulent flows," *Flow, Turbulence and Combustion*, vol. 90, no. 4, pp. 763–783, Jun 2013.

[26] M. Vali, V. Petrović, S. Boersma, J. W. van Wingerden, L. Y. Pao, and M. Kühn, "Adjoint-based model predictive control for optimal energy extraction of waked wind farms," *under preparation for Control Engineering Practice*.

[27] T. Knudsen and T. Bak, "Simple model for describing and estimating wind turbine dynamic inflow," in *American Control Conference*, June 2013, pp. 640–646.

[28] C. Pilong, *PJM Manual 12: Balancing Operations*, 2013, 30th ed., PJM.